Thesis

Evaluation of Interface between Tumor Endoprostheses and Magnetic Resonance Fields

submitted by

Christian Pauritsch

in partial fulfillment of the requirements for the degree of

Doktor der gesamten Heilkunde

(Dr. med. univ.)

at the

Medical University of Graz

executed at the Department of

Orthopaedics and Trauma

under the supervision of

Marko Bergovec, Priv. Doz. Dr. & Andreas Leithner, Prof. Dr.

Gössendorf, 27th of April 2023

Declaration of Academic Integrity

I hereby confirm that the present diploma thesis is the result of my own independent scholarly work. I also confirm that in all cases, where material from the work of others (in books, articles, essays, dissertations, and on the internet) is acknowledged, quotations and paraphrases are clearly indicated. No material other than that cited in the reference list has been used. I have read and understood the Medical University's regulations and procedures concerning plagiarism.

Gössendorf, 27th of April 2023 Christian Pauritsch e.h.

Danksagungen

Ich möchte mich herzlichst bei den Unterstützern dieser Arbeit bedanken, allen voran meinem Diplomarbeitsbetreuer Priv. Doz. Dr. Marko Bergovec, der mich nicht nur beim Verfassen dieser Arbeit unterstützt und angewiesen hat, sondern bereits weit davor bei der Planung, Koordination und Umsetzung der einzelnen Teilbereiche federführend in Erscheinung getreten ist.

Desweiteren gilt mein besonderer Dank allen beteiligten Personen, ohne deren Mitwirken diese Arbeit nicht möglich gewesen wäre: Univ.-Prof. Dr. Andreas Leithner, Priv. Doz. DDr. Maria Smolle, Priv. Doz. Dr. Ursula Reiter und DDr. Igrec Jasminka. Sie alle haben mich sowohl mit Fachwissen unterstützt als auch mit wichtigen Hinweisen unschätzbare Hilfe auf dem mir bis dahin unbekannten Weg der medizinischen Forschung geleistet.

Außerdem bedanke ich mich bei meiner Familie, die mich während der Arbeiten an dieser Diplomarbeit immer wieder motiviert hat.

Zusammenfassung

Primär maligne Knochentumore gehören zu den seltenen Erkrankungen mit zusammengerechnet lediglich um die 8-9 Fälle pro Million pro Jahr.[1] Knochen sind jedoch nicht nur von primären Knochentumoren betroffen, sondern auch andere maligne Tumorerkrankungen wie Prostatakrebs, Brustkrebs oder Lungenkrebs führen häufig zu Skelettmetastasen.[2] Die Behandlung von Betroffenen mit malignen, primären Knochentumoren sowie von Skelettmetastasen ist nicht einfach und verlangt eine multidisziplinäre Herangehensweise bestehend aus systemischer Chemotherapie, Radiotherapie sowie chirurgischer Lokaltherapie.

Für maligne primäre Knochentumore sowie für manche sekundäre Malignome besteht die Lokalbehandlung aus einer weiten Resektion des Tumors mit anschließender Rekonstruktion des Knochens sowie angrenzender Gelenke. In den meisten Fällen erfolgt die Rekonstruktion mittels Tumor-Endoprothesen, die oft auch Mega-Endoprothesen genannt werden. Erkrankte werden nach der Behandlung für Kontroll-Untersuchungen, bestehend aus klinischen und radiologischen Verlaufskontrollen mittels geeigneter Bildgebung z.B. Röntgen, Computer Tomographie (CT) oder Magnet-Resonanz-Tomografie (MRT) einbestellt.

Während der MRT-Untersuchung sind die Patienten und Patientinnen sehr starken und schnell wechselnden Magnetfeldern ausgesetzt. Da die implantierten Tumor-Endoprothesen große und schwere metallische Körper sind, muss mit Wechselwirkungen und Interaktionen dieser Implantate mit den Magnetfeldern gerechnet werden. Aktuell ist nicht bekannt, ob Tumor-Endoprothesen überhaupt sicher für den/die Patient*in unter Einfluss dieser starken Magnetfelder sind. Die vorliegende Arbeit besteht aus mehreren Teilaspekten: Der Implantation von Tumor Endoprothesen in ein Kadaverbein mit Messung der Temperaturveränderungen während der Prozedur, die Untersuchung des Kadaverbeins mittels MRT sowie auftretenden Temperaturschwankungen, das Überwachen von Temperaturveränderungen der Tumorendoprothesen während der MRT-Untersuchung in einem Phantom sowie einem statischen Test zur Bestimmung der Translationskräfte, die in der MRT-Umgebung auftreten.

Im Rahmen unserer Experimente zeigte sich, dass der Implantationsprozess Temperaturdifferenzen von mehr als 80° C verursachen kann. Die anschließenden Messungen der Temperaturschwankungen während der MRT-Untersuchung zeigten keine relevante Erwärmung während verschiedener klinischer Sequenzen. Die abschließend

durchgeführten Messungen am Phantom zeigten ebenfalls für den/die Patient*in klinisch unbedenkliche Werte für Translationskräfte sowie Radiofrequenz-Erwärmung.
Die Ergebnisse dieser Arbeit deuten darauf hin, dass Patienten und Patientinnen, welche eine der getesteten Tumor-Endoprothesen implantiert bekommen haben, zu normalen klinischen Untersuchungen mittels MRT zugewiesen werden können, ohne dass ein relevantes Sicherheitsrisiko aufgrund der Wechselwirkungen zwischen der Tumor-Endoprothese und den auftretenden Magnetfeldern besteht.

Abstract

Primary malignant bone tumors are relatively rare entities with only around 8-9 cases per million per year.[1] However, bones are not only affected by primary tumors but additionally are a frequent site for metastatic disease from other malignant tumor entities like prostate, breast or lung cancer.[2] The treatment of patients being affected by either primary malignant bone tumors or metastatic disease is not easy and calls for a multidisciplinary approach consisting of systemic chemotherapy, radiotherapy as well as local surgical therapy.

For malignant primary bone tumors as well as some secondary tumors, local therapy is done by wide resection of the tumor with consecutive reconstruction of the bone and adjacent joints. In most cases, the reconstruction is done by using a special tumor endoprosthesis, often called megaprosthesis.

Patients undergoing this procedure are subject to stringed follow-up regiments of clinical and radiological examinations using X-ray, computer tomography (CT) or magnetic resonance imaging (MRI). During MRI, patients are exposed to strong and rapidly changing magnetic fields. As implanted tumor endoprostheses are large and heavy metallic objects, interactions with the magnetic fields are to be expected. It is currently unknown if tumor endoprostheses are safe for the patient in the MRI environment.

This study consists of several parts: The implantation of a tumor endoprosthesis in a cadaveric leg with the recording of the temperature changes caused by the procedure, the subsequent imaging of said cadaveric leg using MRI and observation of temperature differences, measuring the temperature changes of the endoprosthesis during MRI procedures in a phantom as well as performing static tests to measure the displacement force exerted during MRI.

Our tests showed increases in temperature up to 80° C during the implantation process. The subsequent testing using the cadaver legs during MRI procedures did not show any clinically relevant increases in temperature. The phantom tests showed clinically irrelevant values for both, displacement force as well as radiofrequency induced heating effects.

The findings of this study suggest that patients who have undergone implantation of one of the tested distal femur tumor endoprostheses may be admitted to MRI without being at risk of danger due the interface between the tumor endoprosthesis and the magnetic fields during this procedure.

1 Inhaltsverzeichnis

2 List of Figures

3 List of Tables

List of Abbreviations

CT: Computer-Tomography
MRI: Magnetic Resonance Imaging
FDA: Federal Food and Drug Administration
ASTM: American Society for Testing and Materials
MR: Magnetic Resonance
SAR: specific absorption rate
E.g.: exempli gratia/for example
GMRS: Global Modular Replacement System
LPS: Limb Preservation System
MUTARS: Modular Universal Tumor and Revision System
CoCrMo: Cobalt-Chromium-Molybdenum (steel)
PMMA: Polymethylmethacrylate
TSE: Turbo Spin Echo
TIRM: Turbo Inversion Recovery Magnitude
VIBE: Volume Interpolated Breathhold Examination
HDPE: High Density Polyethylen
RPM: Revolutions per minute

4 Introduction

Primary malignant bone tumors are a relatively rare occurrence with a cumulated incidence of around 8-9/1 000 000/year.[1] Clinical presentation of affected patients is various and often not very specific. Most of the patients present themselves with local pain and swelling, sometimes accompanied with systemic symptoms like fever, weight loss or reduction of strength.

Generally, the treatment plan for patients diagnosed with primary malignant bone tumors consists of systemic chemotherapy, radiotherapy as well as local surgical therapy.[1] The preoperative planning must take into consideration the exact diagnosis, the localization of the tumor, the feasibility of tumor free resection margins due to tumor tissue spread as well as the patient's wishes. In order to perform a curative local treatment, wide resection margins around the tumor must be achievable without mutilation of the patient and with the added challenge of maintaining the maximal function possible.

Due to the necessary resection margins, a considerable loss of bone, adjacent joints as well as soft tissue must be planned and accounted for when choosing the right method for reconstruction. To enable surgeons to achieve the best possible outcome for the patient, different reconstruction methods can be used. One of the most commonly used reconstruction methods is the endoprosthetic reconstruction using special tumor endoprostheses, often called megaprostheses. These tumor endoprostheses are modular, which means that they can be configurated with different parts and therefore adapted to fit each patient individually.

Treatment of the patients however is not finished even after successful resection and reconstruction, as patients with primary malignant bone tumors are in high risk of local reccurences, which affect around 5,4-10% of patients undergoing limb salvage surgery.[3–6]
In order to detect these local recurrences, a strict follow-up regime is proposed by the European Society of Skeletal Radiology, with radiological examinations every 3-4 months during the first three years after surgery, every 6 months in the fourth to fifth year and annually after that until ten years postoperatively.[3,7]

Different radiological techniques can be used to perform these follow-ups, each one featuring advantages and disadvantages compared to the others. The most common radiological examination method in orthopedics is X-ray.
Easily available and fast, X-ray can be highly beneficial for imaging of the reconstruction site as it is not subject to metallic artifacts around the metallic endoprosthesis. It can be used to evaluate the interface between the bone and the endoprosthesis as well as detect considerable changes in tissue around the operation site. However, it is not a very sensitive imaging method for detection of small local recurrences as it doesn't offer cross-section imaging.[8]

Computer-tomography (CT) is another frequently used imaging method. It offers highly detailed three-dimensional imaging of boney structures with the added benefit of being able to spot smaller soft-tissue changes than X-ray. This method suffers from metal artifacts around metallic implants, degrading its sensitivity.[8]

Magnetic resonance imaging (MRI) is the most sensitive imaging method to detect changes in soft tissue due to its unparalleled soft-tissue contrast. Like CT, it offers three-dimensional imaging and is subject to metal artifacts around metallic hardware.[7,8]

In addition, MRI method poses a unique challenge. It necessitates the exposure of a patient to very strong magnetic fields with magnetic forces exceeding the earths gravitational field thousandfold.[9] While this usually is not a concern for human beings as the human body is generally diamagnetic[10], the magnetic forces can be a safety hazard for any metallic body brought into proximity of the MRI apparatus.

This consideration is especially true for any metallic objects implanted into a patient's body. As a result, any metallic object routinely implanted into a patient's body must be tested and labeled according to the U.S. Federal Food and Drug Administration (FDA).

Labelling categories are:

MR safe
MR unsafe
MR conditional[11]

Testing must be performed according to the recommendations by the American Society for Testing and Materials (ASTM). Not every device must be tested individually, as a device can be deemed “MR conditional” using a scientific rational instead of explicit testing for example if it is made from a material which has proven to have insignificant interactions with the magnetic field in similar devices.[11]

For tumor endoprosthesis however, it is not known if they are MR safe, MR unsafe or MR conditional. While public registers exist for a variety of orthopedic and other implantable devices, the MR safety status of these tumor endoprosthesis is unknown.

As patients who have undergone implantation of these devices are subject to the aforementioned follow-ups and are therefore much more likely to be exposed to the strong magnetic forces in the MRI environment, there is a high need to assess and define the safety of tumor endoprostheses within the MRI fields.

The aim of this thesis was to evaluate the possible interface between tumor endoprostheses from different manufacturers and the magnetic fields occurring in the magnetic resonance environment and assess possible implications for patient safety during magnetic resonance imaging procedures. In addition, a cadaver study of the implantation process was performed to identify critical moments during the procedure which may cause excessive heat distribution at the bone, which could cause thermal necrosis of the bone and in turn could be a contributing factor to the consequent failure of the tumor endoprosthesis.

At the time of writing, no article regarding the safety of tumor endoprostheses has been published on PubMed.

4.1 Magnetic Resonance Imaging

Magnetic resonance imaging works by taking advantage of a basic physical principle: the “spin” of atoms, or rather the spin of the cores of hydrogen atoms. As these spinning cores have a very small electrical charge, their rotation in combination with this electrical charge

creates a magnetic field around the atom, with the orientation of the magnetic field lines running through the spin axis.[9]
As the orientation of these small magnetic fields in tissue is random and therefore effectively neutral, they need to be oriented along a known axis by bringing them into a static magnetic field. The magnetic field used for medical imaging is called B_0 and its strength is dependent on the MRI apparatus, with most of the models currently in clinical use being able to produce field strengths of 1,5-3 Tesla.[9] Ultra -high field strength MRI with 7-9T is not very prevalent in clinical use as of time of writing.[12,13]

When being exposed to the B_0 field, only fraction of all of the hydrogen cores can be oriented along its magnetic field lines, with the surplus of oriented atoms to unoriented atoms depending on the field strength of the apparatus. To be able to produce a picture however, these cores need to be „flipped“, therefore being brought out of alignment with the static B_0 field.
The flipping is done by using high frequency transmitters, which create a perpendicular magnetic field B_1 to the B_0 field. The strength and length of the B_1 field influences the resulting “flip-angle”, with the length of high-frequency pulses usually being around 0,5-5ms.[9]

After being flipped and being brought off axis, the hydrogen atoms will try to go back into alignment with the static field. The time it takes these protons to reach realignment is called relaxation time, which can be measured and used to differentiate between tissues as every tissue has a specific relaxation time and density of hydrogen cores.[9]

To create an image which can be used for medical purposes, additional magnetic fields must be utilized to add spatial information: gradient fields, which can alter the magnetic field in a specific location, so that the radiofrequency pulses only affect this specific area.

These gradient fields are relatively weak in comparison to the static B_0 field, with a strength of around 40mT/m (depending on the field strength of the MRI apparatus), but are switched on and off in very rapid cycles with durations of down to 1ms.[10,14]
By using gradient fields along all directions with the z orientation coding for the layer, the x axis for frequency and the y axis for the phase, images can be produced by repeating the imaging process for each of the voxels in the image.

4.1.1 Safety concerns of magnetic resonance imaging

The physical principles behind magnetic resonance imaging call for a very strong static magnetic field as well as rapidly changing high frequency magnetic fields and fast changing gradient fields. This variety of magnetic fields are the cause for different safety concerns, as every material has magnetic properties.
Some of the safety concerns are especially important when it comes to bringing foreign metallic bodies like orthopedic implants next to or even into the magnetic field of a MRI machine. Regarding the interface between magnetic resonance fields and metallic objects, two main safety aspects can be differentiated: the interaction of metals with the strong static field and heating effects caused by the high frequency fields.[15]

4.1.1.1 Static field and magnetism

As previously mentioned, every material interacts with magnetic fields to a certain degree. This phenomenon is called „magnetic susceptibility“. The general direction of this susceptibility of different materials can be divided into two main categories: positive and negative. When a material is being exposed to an external magnetic field like those created by MRI machines, it creates its own magnetic field. The difference between these two clusters is the orientation of this resulting magnetic field.
Generally, three different clusters of magnetic behavior can be distinguished[10]:

- Diamagnetic materials (e.g. water, plastics, wood) have a negative susceptibility. When exposed to external magnetic fields, these materials create their own magnetic field oriented against to the external magnetic field.[15] This results in a very insubstantial repulsion effect.[10]

- Paramagnetic materials on the other hand produce a small magnetic field which increases the strength of the external field slightly. The resulting added magnetic field is usually too small to be of great concern. Paramagnetic properties of different materials can be used for imaging with contrasting agents or for functional MRI scans, where the paramagnetism of deoxyhemoglobin is used.[10]

- Ferromagnetic metals (iron, nickel, cobalt) amplify the magnetic field surrounding them to a great extent by being able to become magnetically saturated. This saturation is caused by alignment of all the molecular dipols with the external magnetic field, causing a large local magnetic field[10]. These materials can even remain in a magnetized state after the causing magnetic field is no longer active.[15]

Therefore, metallic bodies made from ferromagnetic metals or metallic alloys containing iron, nickel or cobalt, are subject to potentially very strong interactions of with magnetic fields, the following safety aspects have to be considered when it comes to bringing them into the magnetic resonance imaging environment:

4.1.1.1.1 Translational forces

Translational forces experienced by magnetic bodies depend greatly on the homogeneity of the magnetic field surrounding them. If the surrounding magnetic field is homogenous, no translational forces are exerted on the metallic body.
This changes if the magnetic field is inhomogeneous. The inhomogeneity results in translational forces oriented in the direction of wherever the magnetic field is stronger.
In MRI machines, the magnetic field inside the bore is homogenous, but changes naturally at the gantry, where the spatial gradient (the change in the strength of the magnetic field in relation to the distance to the scanner) is the largest.[10] The orientation of the spatial gradient at the gantry is towards the center of the bore, with a stronger magnetic field inside the bore of MRI apparatus when compared to the outside.[15]

As a result, translational forces would be directed towards the center of the MRI machine, where the field strength is the greatest.[15] With sufficient strength of the static magnetic field, the resulting translational forces could result in a projectile effect, which in return can be a cause of injury to a patient.[16]

The attractive force exerted onto a metallic object made from iron can be significant and change drastically within proximity of the scanner, ranging from translational forces around

the weight of the object at around 1m distance to the apparatus to more than a hundred times the weight of the device within this distance.[10]

4.1.1.1.2 Torque

Torque is induced when an object with sufficient magnetic properties tries to align its magnetic axis with the magnetic field lines of the surrounding magnetic field.
Alignment results in a rotational movement and unlike translational forces, it is not influenced by the homogeneity of the surrounding field but only on the relative orientation of the magnetic axis to the field lines.
The torque is dependent on the length of the device, longer devices create greater torque.[15]
Counterintuitively, the force needed to keep a device under the influence of magnetically induced torque from spinning is larger for shorter objects. This means that the force tissue surrounding a metallic body must withstand to prevent torque is greater for smaller implants than for larger, heavier ones.[10] This phenomenon can be highly relevant with vascular clips, as rotational movement could result in damage to blood vessels.[15]
For smaller devices, the induced torque can be of greater significance as a safety concern than potential translational forces, as the needed force to keep a device from rotating can be a multitude of the translational forces.[10]

4.1.1.2 Radiofrequency induced heating

Thermal heating effects can be caused by the radiofrequency field, as the energy carried by these frequencies can be absorbed in tissue.
Energy deposition within any material (in the case of medical magnetic resonance imaging bodily tissue) results in a rise in internal energy, which in turn leads to an increase in temperature. The amount of energy deposition per mass of tissue is measured in SAR (specific absorption rate) and is usually given in watts per kilogram (W/kg).[16]
Although only specific body parts are exposed to an increased energy deposition during magnetic resonance imaging, even a localized increase in temperature would consecutively result in a rise in overall core body temperature due to transportation of thermal energy by the blood flow. To prevent health and safety concerns, the maximum specific absorption rate is limited to 4 W/kg for whole body examinations.[15,16]

In metallic objects however, the rapidly changing radiofrequency fields used during magnetic resonance imaging could lead to increased energy deposition. This is the result of the different and much higher conductivity of metals when compared to human tissue.[15]
This phenomenon is called “antenna effect” and together with the magnetic gradient fields, which also could lead to resonance effects depending on the length of the metallic device, the changing magnetic fields could result in thermal damage to bodily tissue.[17]
The extent of the heating effect is dependent on resonance effects. These in turn are highly dependent on the wavelength of the radiofrequency fields.
Increased heating of implants has been shown to occur primarily when the length of the device is around half of the wavelength of the excitation frequency, the frequency of which corresponds with the field strength of the MRI apparatus. Field strengths in clinical use have a excitation frequency of around 64 MHz for 1,5T, 128 MHz for 3T.[9] Multiples of these frequencies could also contribute to excessive heat deposition.[15]
The wavelength of a 64 MHz wave is around 4,7 m in air[15], which would call for a 2,35 m long orthopedic device to be subject to the antenna effect mentioned above, making it effectively negligible. However, the wavelength changes drastically depending on the medium the wave is traveling in, as the speed of the radiofrequency wave is different. For fat or water, the wavelength is reduced to a around a third for 1,5T MRIs, respectively to a nineth of this distance for 3T MRI machines.[15]

Longer orthopedic devices with corresponding length could therefore be subject to the antenna effect, which can induce electric currents with a very high voltage. As the metal endoprostheses are better at conducting electricity than the surrounding bodily tissue, the difference in conductivity results in an increase in temperature at the transitional areas, where suddenly the conductivity changes. This is mostly true for the ends of the stems of the endoprostheses.[15]

An additional aspect to consider regarding metallic devices in the magnetic resonance environment is the occurrence of susceptibility artifacts, which are caused by a sudden difference in susceptibility at the interfaces between different materials (e.g. soft tissue/bone). This is especially true for the interface between human tissue and metal. With normal gradient fields, the error resulting from such metallic interface can be large enough to cause eradication of adjacent structures, so called „drop out“.[14]

1.1.1.3 Gradient fields

As previously mentioned, the gradient fields are much weaker than the static magnetic field B_0. The main safety concern when it comes to patient safety regarding these moderate magnetic fields comes from their loud noises, as the Lorentz force exerted on the copper wires during these short power bursts is considerable and can reach loudness levels of up to 130 dB.[10] In addition, they can reach the necessary threshold for the stimulation of peripheral nerves due to induced electricity. In magnetic resonance machines with very strong gradient field generators of more than 300 mT/m the stimulation of cardiac cells is theoretically possible.[10]

4.2 Malignant primary bone tumors

Primary malignant bone tumors do occur across all age groups[5,18], with the most common types of these malignant bone tumors primarily affecting children, teenagers and young adults. These tumors are relatively rare, with a combined incidence rate of around 8-9/1 000 000/year, with no entity itself accounting for more than 2-3/1 000 000/year.[1]

The most common entity of these primary malignant bone tumors are osteosarcomas, with an incidence of around 3/1 000 000/year. The age group affected the most are young adults between 15-19 years.[19,20]
Osteosarcomas a predominantly located in the long bones of the extremities, with the most common anatomical site being the knee[1]. However, also older patients can be affected, with a second peak round the 7th to 8th decade.[18]
The second most common malignant primary bone is Ewing´s sarcoma, with an incidence of 3/1 000 000/year. As with osteosarcoma, the primary age group affected are children and young adults.[21,22]
Ewing sarcoma develops out of mesenchymal cells and not osteoblasts, therefore patients may not only present themselves with sarcomas originating from bone, but also with soft-tissue origins in around 25-30% of cases.[1,21]

For adults, chondrosarcoma is the most common entity of primary malignant bone tumors with an incidence of 2/1 000 000/year.[1] Chondrosarcomas may not only arise as a de-novo

lesion (primary chondrosarcoma) but also as a malignant transformation of a previously benign cartilaginous tumor like enchondroma (so-called secondary chondrosarcoma).[1]

As the treatment of these sarcomas calls for a multidisciplinary approach, admission to specialized care centers is highly advised. Treatment usually consists out of treatment regimens with systemic chemotherapy, local therapy and radiotherapy. If curative treatment with excision of the tumor is regarded to be achievable, chemotherapy and consequent surgery should be used.[1]

Local surgical therapy should be performed after neoadjuvant chemotherapy is done. The goal of adequate resection is the removal of the tumor "en-bloc", resulting in tumor free resection margins (so called R_0 resection). Therefore, local surgical therapy results in a major conflict: the wider the resection margins the safer it is to achieve a R_0 resection and therefore a safer oncological outcome. At the same time, wider resections result in a greater loss of overall function of the affected area.
For the distal femur for example, any soft tissue components of a tumor within the quadriceps muscle necessitate resection of at least a part of said muscle with a consecutive loss of function of the extensors in the knee. However, achieving R_0 margins is highly important for the oncological outcome and therefore should outweigh the concerns for function.[23]

If adequate resection margins are not achievable, amputation of the affected limb can still be a feasible option, with comparable overall survival.[23] If surgery is not possible, definitive radiotherapy only may be used.[24]

The same statement is also true for Ewing sarcoma. Local control of the tumor may be done by surgical removal of the tumor with radiotherapy. The procedure should be performed if the local situation allows for tumor free margins and acceptable quality of life as well as function. If surgery is not possible, definitive radiotherapy can be considered.[1]
However, surgery showed to have significantly lower local recurrence rates when compared to treatment using only local radiotherapy.[22] Furthermore, the combination of surgery and radiotherapy showed lower local recurrences than surgery alone.[22]

With the use of chemotherapeutic regiments and advances in surgical approaches, the survival rate of primary bone tumors has increased significantly raising from 10-20% to 60-80%.[1,22,24]

As mentioned in the introduction, patients who have undergone limb salvage surgery are subject to a strict follow-up regiment consisting of clinical and radiological evaluation. Suitable imaging modalities for follow-ups are standard radiography, MRI as well as CT scans.[25]

4.3 Tumor endoprostheses

Before the development and availability of adequate chemo- and radiotherapy, limb amputation was the surgical treatment of choice. Nowadays, due to the availability of multidisciplinary treatment, limb-salvage surgery can be a viable option in up to 90% of cases.[26] However, amputation may still be used as an alternative to limb-sparring procedures for patients which are too young for surgery or where the necessary resection margins cannot be achieved otherwise[26]. Different studies have shown that the overall outcome regarding survival as well as quality of life is comparable between limb salvage and amputation.[23,26]

Limb-salvage surgery treatment can be divided into endoprosthetic and biological reconstructions following the resection.

Biological reconstruction can be done using bone allo- or autografts, with the aim to restore the loss of boney structures with either autologous donor bone and/or allograft bone from the bone bank.[5,26]

The endoprosthetic approach uses specialized tumor endoprostheses, which allow for the necessary safe resection margins and can be adjusted to account for the resulting loss of bone tissue. As standard endoprostheses cannot be used for this purpose, tumor endoprostheses offer the benefit of “in-operation” adaption of length and torsion, resulting in adequate fit and overall outcome for the patient.[27,28]

While originally designed for tumor surgery, most of the tumor endoprosthesis systems can also be used for revision surgery and trauma, for example when aseptic loosening causes the failure of a standard knee replacement. Most of the tumor endoprostheses in clinical use are modular systems. They can be adapted in length by adding extension pieces of different dimensions between the stem and the articulating joint to achieve the resection margins necessary.
Additionally, these modern modular endoprostheses experience a significantly lower mechanical failure rate than previously used, custom-made implants, which were often cast from titanium alloys.[29]

4.4 Complications of tumor endoprostheses

Despite their frequent use, tumor endoprostheses have a very high rate of complications, ranging from 24.5% to 43% depending on location, with the mean time to failure being forty-seven months but varying for different anatomical locations and failure modes.[30–32] This is put in context when compared standard knee replacements which have revision rates around 3-5% within a 10 year timespan.[33]

The drastic differences in number of complications when comparing standard knee endoprostheses to tumor endoprostheses can be attributed to several possible factors, with some of them being for example longer operation times, larger surgical access sites and higher blood loss.[27] Additionally, complications are higher when radiotherapy and/or neo-/adjuvant chemotherapy are used.[31]
Due to the high number of complications and failures, a specialized system for the classification of such failures was proposed in 2011 by Henderson et al.[30]
His team proposed two main clusters for classification, mechanical and nonmechanical. Mechanical was further divided into soft-tissue failure, aseptic loosening and structural failure. Nonmechanical failure modes are infection and tumor progression.[30]

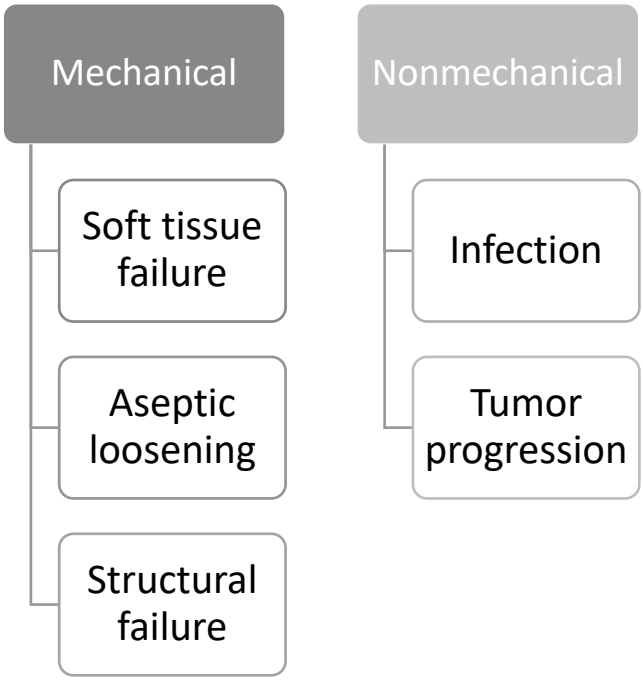

Fig. 1 Classification mode of complications of tumor endoprostheses after Henderson et al. 2011

Their study population showed that the most common type of failure was infection, which according to said classification system is considered a nonmechanical failure and accounted for 34.1% of all failures across all anatomical reconstruction sites.[30]

The second most common failure mode according to their research was aseptic loosening, considered a mechanical failure and was the reason for endoprostheses failure in 19.1% of cases. Across all cases, the failure rate of primary procedures was around 29%.[30]
Research performed by other authors backs their findings, as infection consistently is one of the most common causes for tumor endoprosthesis failure.[31,32,34,35]

Aseptic loosening is of great concern for other authors as well, being the main cause for failure of tumor endoprostheses in around 5-10% of cases.[34] While the failure rate is high, failure of the tumor endoprosthesis itself (e.g., breakage of hinge or breakage of material) is relatively rare, with a 15-year survival rate of the prosthesis at around 93.7%.[29]

In addition, advancements in endoprosthesis design can potentially lower the risk of complications. For example, polyaxially hinged joints demonstrated significantly lower complication rates than hinged joint designs.[30,34] Antibacterial coatings like silver also seem to reduce the rate of early infections.[34] Different stem designs have also shown to improve

the overall survival of the endoprosthesis as anatomically curved stems resulted in better anchorage in the bone when using uncemented stems.[34] Different brands have tried to incorporate these findings into the design of their tumor endoprostheses, with some brands featuring polyaxially hinged joints and special stem designs and coating.

4.5 Brands tested

For the purpose of this study, we chose the three most commonly used tumor endoprosthesis. All of these systems are modular, available off-the-shelf and easily available worldwide for the reconstruction of bone and joints due to surgery.

4.5.1 GMRS

GMRS (Global Modular Replacement System) by Stryker (Kalamazoo, USA) was the successor to the HMRS and put into use in 2003. The HMRS in turn was the successor of the first modular endoprosthesis system, called the KMFTR (Kotz Modular Femur and Tibia Reconstruction System). The main differences between the earlier version HMRS and the GMRS was a change to a modular rotating hinge design of the distal femur/proximal tibia.[36] The stems and extension pieces are made from titanium and cobalt chromium (CoCr) alloys.[27]

4.5.2 LPS

The LPS (Limb Preservation System) by Depuy Synthes (West Chester, USA) uses different modules in 5mm increments to allow for precise adaption of the required length.[27]
While the extension pieces are made from titanium alloys and are fitted together using a taper lock design, the distal femur articulating component is made from cobalt chromium (CoCr) alloys. The distal femur is connected to the proximal tibial component via a rotating hinge design.[34]

4.5.3 MUTARS

MUTARS, (Modular Universal Tumor and Revision System) is the newest system out of the tested modular endoprostheses and is made by Implantcast (Buxtehude, Germany).
This system was introduced in 1992 and developed by Implantcast in collaboration with Prof. W Winkelmann and Prof. G. Gosheger from the Department of general Orthopaedics and Tumor Orthopaedics at the University Hospital in Munster. The system uses different alloys for construction, namely Implavit® and Implatan®. Implavit® is a titanium alloy (TiAl6V4) while Implatan is a stainless-steel alloy made out of cobalt, chrome and molybdenum (CoCrMo).[27] The MUTARS system uses a hinged-joint for coupling the distal femur to the proximal tibia.

Fig. 2 Left to right:

1: MUTARS *2: LPS* *3: GMRS*

5 Materials and Methods

For this thesis, two independent experiments were performed to evaluate the amount of interface between tumor endoprostheses and magnetic resonance fields occuring during magnetic resonance imaging procedures. As test specimen and further evaluation, distal femur tumor endoprostheses were chosen, as the distal femur is the most common site for malignant primary bone tumors needing resection and subsequent reconstruction using tumor endoprosthesis.[37]

The first experiment was a cadaver study to not only evaluate the risks and dangers to the endoprosthesis hold during the implantation process of tumor endoprostheses but furthermore the measurement of the amount of interface between the endoprosthesis and the magnetic resonance fields during imaging in a nearly in vivo like condition.

The second part was primarily focused on MRI safety and consisted of two different experiments which were performed according to the testing protocols predetermined by the ASTM. We followed the guidelines for two safety aspects, radiofrequency induced heating and magnetically induced displacement force.

This study was approved by the ethics committee of the Medical University of Graz with the EK-number 31-169 ex 18/19.

5.1 Cadaver Study

5.1.1 Implantation

The first test performed was a human cadaver study. As adequate test subjects, two lower extremities (both right side) were obtained from the Institute of Anatomy from the Medical University of Graz.

Both tested extremities were conservated using Thiel´s method, which results in a relatively "in vivo" tissue density as well as comparable moisture content. A simulated knee replacement was performed on both legs using MUTARS tumor endoprostheses for the

distal femur and the tibial plateau with the according stem. The resection length and subsequent tumor endoprosthetic reconstruction was 10 cm of distal femur. One lower extremity underwent implantation of a tumor endoprosthesis with an uncemented stem design for the proximal as well as the distal stem.

The second lower extremity was implanted with cemented stem designs for the distal femur as well as the proximal tibia. The bone cement used for this procedure was a PMMA bone cement Palacos© (Heraeus Medical GmbH, Wehrheim, Germany). The procedure was performed precisely as it would be on a normal patient using the same materials and methods as stated in the MUTARS Distal Femur Surgical Guide. The process was frequently interrupted to measure the temperatures resulting from the operation. Measurements were taken using four LumaSense Technologies Flouroptic® temperature probes and TrueTemp3.0 software on a windows personal computer.

Our aim was to assess and identify the critical moments for bone integrity, which could potentially later be a contributing factor to complications such as aseptic loosening of the implant. The critical temperature not to exceed is 51°C, a value which is generally accepted to be the temperature at which the alkaline phosphatase starts to denaturalize.

Critical moments of the procedure were assessed and discussed beforehand and included:

- Osteotomy of the femur
- Osteotomy of the tibia
- Use of drills and reamers to prepare the bone for the implantation of the stems
- Use of bone cement for the cemented stem designs

While using power tools, measurements were taken from the tool itself (tip of the saw, drill, reamer) as well as the bone area directly affected by the tool (cut edge, edge of reamed hole, etc.) and surrounding tissue (bone and soft tissue).

To measure the temperature of the bone cement while hardening, holes were drilled into the bone in advance. Drilling locations were at the proximal end of the femoral stem, the distal femur close to the articulating joint as well as the end of the tibial stem.

This procedure enabled recording of the temperature of the bone cement while hardening inside the bone in a representative thickness.
Simultaneously, a reference ball formed out of the same bone cement with a diameter of roughly 30 mm was monitored using the fourth probe.

Fig. 3 Measurement of cement hardening during cementation of the distal femur tumor endoprosthesis. Measurements were compared to a reference ball formed from the same bone cement.

5.1.2 MRI Measurements

After the implantation, the lower extremities were transferred to the Department of Radiology at the University Clinic of Graz.

Successively, both legs were placed into the 3T MRI (Siemens Magnetom Skyra).
Fiberoptic temperature probes (Luma Sense) were attached into the aforementioned pre-drilled holes in the femur for the two stems (femoral and tibial stem) as well as at the contact between the tumor endoprosthesis and the femur and the articulating joint.

Sensor	Temp 1	Temp 2	Temp 3	Temp 4
Position	Tibial Stem	Articulating Joint	EP/Femoral Contact	Femoral Stem

Table 1 Sensor Positioning During Cadaver Evaluation of Radiofrequency Induced Heating

A series of standard imaging protocols was performed during which the temperature at each of the testing locations was recorded every 5 seconds using the same TrueTemp3.0 software.

The series of imaging protocols included standard knee and hip imaging as well as artifact suppression protocols. The metal artifact suppression protocols would normally be used to reduce the artifacts created by the distortions of the magnetic field around the metallic objects due to susceptibility artifacts.

In addition, a scenario where a patient would undergo magnetic resonance imaging for completely tumor and follow-up unrelated medical reasons was included by running a variety of different standard clinical imaging protocols (TSE, TIRM, VIBE DIXON).

To account for different possible conditions during imaging, some of the sequences were performed with a body coil placed over the cadaver legs, while others were performed using a knee coil. For other imaging sequences, no coil was used.

5.2 Phantom Testing

For the second part of this experiment specifically constructed phantoms and fixtures were planned, constructed and subsequently tests performed according to the protocols given by the ASTM with a special focus on two of the different possible safety dimensions.
Two main safety aspects were assessed:

- Magnetically induced displacement force
- Radiofrequency induced heating

The third possible safety aspect, magnetically induced torque, was not measured according to ASTM protocols.

All the measurements were taken with the tumor endoprostheses being configured as they would be for a patient undergoing implantation after surgical removal of boney structures to allow for 10 cm of resection margin for the distal femur and subsequent endoprosthetic reconstruction using the respective tumor endoprostheses.

5.2.1 Radiofrequency induced heating

For a precise measurement of radiofrequency induced heating, a phantom which was later filled with gelatine as well as a supporting structure to secure the implants and the temperature probes had to be constructed.

5.2.1.1 The phantom

The ASTM protocol specifies two versions of the imaging „phantom“ which is an open container made of MR safe materials. This container is supposed to be filled with a gelatine solution with the same conductivity as human tissue.
The standard version has a rectangular footprint of 65 x 42 cm with a wall height of 9 cm. If this area is insufficient to allow for larger objects with the necessary distance to the walls, another rectangular area with a footprint of 27 x 15 cm can be added in the middle of the shorter side.
For our tests a container with the extended footprint was constructed out of 8 mm thick extruded acrylic glass (Plexiglass®), however, the additional footprint and area was not necessary and therefore blocked off before filling the phantom with gelatine.
As the tested device must be a minimum of 1,5 cm away from each of the walls as well as to the surface and the bottom of the gelatine, the height of the phantom can be varied. As the tested tumor protheses are broader at the articulating joint, the phantom was constructed with a 15 cm wall height instead of 9 cm to achieve a higher fill level. The gel used to submerge the endoprostheses in was ultrasonic gel (Henry Schein) instead of the preformulated one in the ASTM protocols. This allowed for a longer shelf life while providing similar resonance properties as human tissue.

In total 30 kg of gel were used. This resulted in a fill level inside the phantom of around 10 cm. This was adequate to keep the necessary distance to the surface and bottom of the phantom after placing the prostheses inside the phantom.

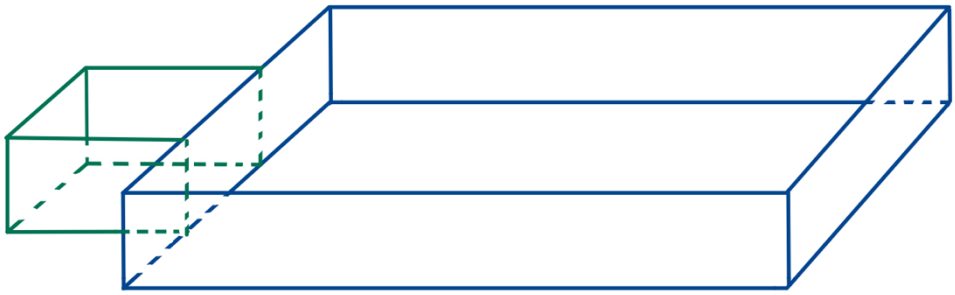

Fig. 4 Phantom Schematic
Blue Area= 65 x 43cm
Green Area (optional) = 27 x 15cm

5.2.1.2 The fixture

The supporting structure used to hold the endoprostheses as well as the fluoroptic temperature probes in place during the imaging procedures was made of acrylic glass, nylon screws and HDPE rods. As specifications of tumor endoprostheses differed between manufacturers and systems, the structure had to be adjustable to be able to support the different systems while also providing accurate and repeatable placement of the temperature probes during measurements. The bulk of the structure was made from 3 mm extruded acrylic glass (Plexiglass®) and featured two rails along which the supporting structures for the endoprostheses and the temperature probes could be moved and fastened to allow for different lengths and heights.

The tumor endoprostheses were supported by four implant holders made from bodies out of 2 cm thick acrylic glass, with a through-drilled channel in which height adjustable high-density polyethylene (HDPE) rods could be placed.
On top of these rods, 1,5 mm thick acrylic U-shaped holders were mounted.

The thickness of the contacting acrylic structures is not irrelevant as according to ASTM protocols the sensors must be placed at least 2x the support thickness away from the support structure.

Therefore, using a thinner material allowed for more flexibility for temperature probe placement[38]. The four temperature probe supports were built from the same acrylic and HDPE materials. Height adjustment was achieved by using a locking feature using nylon screws, the temperature probe was locked in place in a channel running through the HDPE rods.

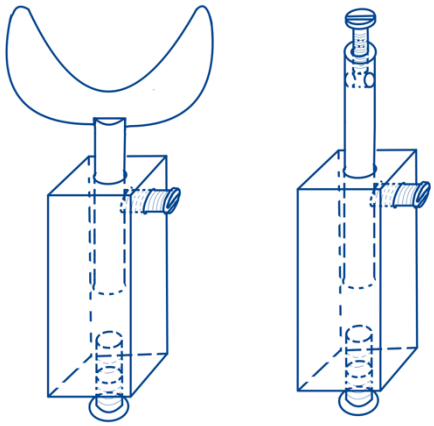

Fig. 5 Schematic: Tumor Endoprosthesis Support (left) and Temperature Probe Support (right)

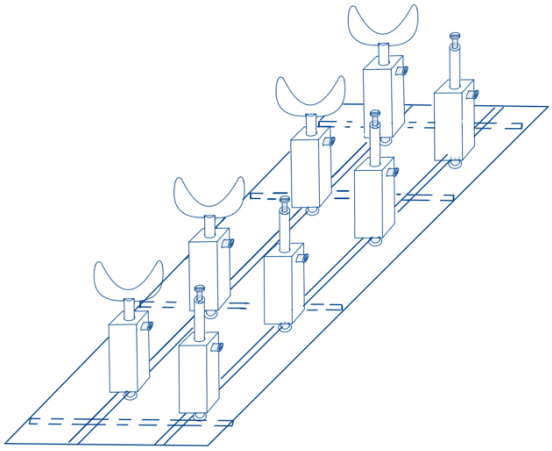

Fig. 6 Figure 6 Schematic: Supporting Structure on Mounting Plate

5.2.1.3 The sensors

For recording the temperature, four LumaSense Technologies Flouroptic® temperature probes were used and placed at the locations which were expected to experience the highest increase in temperature.

The probes were connected to a computer running TrueTemp 3.0 software to record temperature data of all four probes every 5 seconds during testing.
The recorded data points were then saved as .txt and exported into Microsoft Excel. This data was then exported to SPSS for further analyzation and statistics.

Test locations:

Probe 1	Femoral Stem
Probe 2	Articulating Joint
Probe 3	Tibial Stem
Probe 4	Reference

Table 2 Temperature Probe Placement During Phantom Testing

Probe locations were chosen due to the underlying physical principles previously discussed. The stems with their long, tubular shape may be subject to interferences with the rapid changing radiofrequency fields as well as the gradient fields.
The articulating joint on the other hand is not only the center of mass due to its high metal content and weight, but depending on manufacturer also made from chromium molybdium steel (CoCrMo) and therefore contains at least some amount of paramagnetic as well as ferromagnetic materials. As the precise formulation of these alloys is dependent on the manufacturer and also not publicly available, there might be variations between the different systems.

To adhere to the ASTM protocols, the reference probe was placed and oriented to face only the gelatine and a minimum of 10cm away from the endoprostheses at a similar height to allow for comparable SAR.
Before each test run, the temperature probes were calibrated to the current room temperature.

5.2.1.4 Test Procedure

Before testing, all prosthesis were placed in the examination room for two hours to reach temperature equilibrium. Similarly, the phantom was placed in the examination room one hour before testing to allow for assimilation of temperature.

Firstly, the endoprostheses were submerged one after the other in the gel filled phantom and the supports adapted to support the specific specimen for the procedure.
Consequently, the temperature probes were placed adequately to record the temperature at the testing locations given in Fig. 2. Then, the phantom was placed on the examination table and aligned with the center of the MR apparatus. Before testing, the temperature probes were calibrated at the current room temperature (~22° C).

In accordance to the ASTM protocols, a 15-minute „worst-case-scenario“ with a maximum SAR of 2 W/kg and rapidly changing radiofrequency fields was performed. This procedure is expected to result in the greatest heating effect if any occurs. This SAR value exceeds the standard amount of absorption rate during standard imaging (around 0,6 W/kg).

Additionally, a series of standard clinical protocols for knee and hip imaging using different sequences consisting of 10 sequences (TSE, TIRM, VIBE DIXON) were performed to imitate a more realistic situation, as patients undergoing implantation of tumor endoprostheses may be subject to magnetic imaging during tumor unrelated joint imaging.

Additionally, the same sequences were performed with the endoprostheses being upheld in air instead of gelatin, to evaluate if this would result in a different overall outcome in recorded temperatures, as the effect of radiofrequency induced heating is largely dependent on resonance effects which in turn depend on wavelength. Different media in could therefore change resonance effects and influence the recorded temperatures.

5.2.2 Displacement Force

5.2.2.1 The Fixture

The fixture to measure the displacement force was made from a sturdy wooden frame. The tumor endoprostheses were suspended from this structure using a lightweight string. To measure the resulting angle of displacement, a goniometer was attached with the 0° mark oriented at the swivel point of the string. According to ASTM protocols, the string used must be lighter than 1% of the weight of the tested device, as to not cause relevant errors for the calculation of the resulting displacement force.
As the string in our study had to support a weight of around 1,4 kg, we used 2.0 Supramid (30 cm length) with a weight of approximately 1,5 g (around 0,1% of the weight of the tested devices). To increase the contrast to improve readability of the attached protractor and therefore the displacement angle, a sheet of paper was attached.

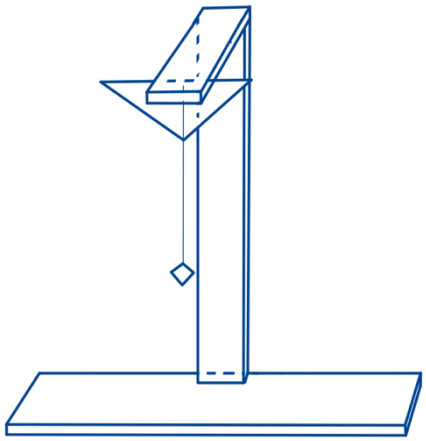

Fig. 8 Schematic: Displacement Force Fixture

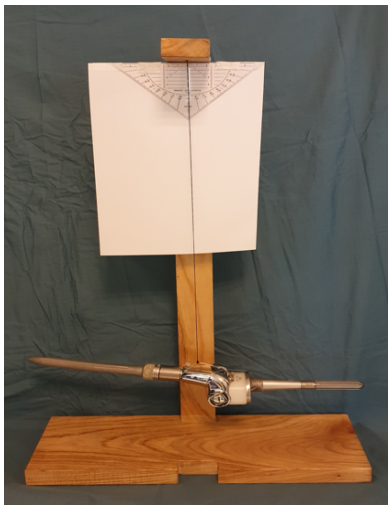

Fig. 7 Displacement Force Fixture with Tumor Endoprosthesis (GMRS) in Testing Configuration

5.2.2.2 Test Procedure

To measure the displacement force, the fixture was placed within the MRI apparatus to align the tumor endoprostheses with the centre of the bore, as there the greatest amount of displacement force is expected to be exerted by the static B0 field due to the greatest change in homogeneity at the entrance. Ordinary tape was used to mark the proper fixture placement to enable repeatable measurements and allow for consistent positioning after switching out the tumor endoprostheses.

Before being placed into the bore of the MRI apparatus, each tumor endoprosthesis was weighted using a household scale (Soehnle, Nassau) with a precision of 1g. This accuracy was adequate for the test.

To be able to attach the tumor endoprostheses in a horizontal orientation, each one was attached by using a supporting harness made from lightweight nylon string. This was done intentionally, as these orthopaedic devices typically would be positioned in magnetic resonance fields this way with patients usually lying on the examination table. Therefore, the resulting displacement forces could be observed under more realistic conditions.

After positioning the endoprostheses accurately and adjusting the examination table to be as close to the bore entrance as possible, the resulting displacement angle was read by three different individuals.

The mean angle resulting from the three angles was then used for calculation.

The resulting displacement force is then calculated using following formula as given in the ASTM protocol:

$$\boldsymbol{Fm = \tan(a)\ x\ m\ x\ g}$$

Where:

Fm: Displacement force exerted by magnetic fields

tan (α): tangent of observed deflection angle

m: Mass of the tumor endoprosthesis in SI (kg)

g: Gravitational force (≅ 9,81m/s)

Test Specimen	Endoprosthesis Weight (kg)
MUTARS	1,256
GMRS	1,315
LPS	1,392

Table 3 Weight of tested Tumor Endoprostheses with proximal femoral stem, one extension piece, distal femur component, insert, tibial component and tibial stem with a combined length of approximately 35cm (see Fig. 2 for reference)

During this experiment, the resulting alignment with the static magnetic field was observed as well. This alignment is the result of torque being exerted by the magnetic field. The faster the endoprostheses align themselves with the magnetic field lines, the more torque is exerted on them. In some publications[39], this phenomenon of alignment is graded in numbers 0-4, with 0 being no observable alignment with the magnetic field and 4 being violent and abrupt alignment.

6 Results

6.1 Cadaver study

6.1.1 Implantation

During implantation, several measurements during the use of power tools showed vast increases in temperature over the baseline thermometer readings.
The greatest increase in temperature was observed directly after femoral reaming using a fixed reamer.
The recorded temperature at the tip of the tool was 122°C, an absolute increase of around 100°C from base temperature of around 21°C. Femoral osteotomy also proved to increase the tissue temperature considerably with 74,2°C measured at the femoral osteotomy site.
The PMMA bone cement that was used for securing the cemented endoprosthesis inside the bone did not show an increase in temperature of more than 6°C, while the reference cement ball did heat up to more than 120° C at the measurement point.

Action	Temperature	Sensor
Referencing	22° C	1-4 (Cadaver)
Femur osteotomy	50° C	2
Tibia drilling	52° C / 47° C	1 (tibia) / 2 (drill)
Tibia osteotomy	22°C	2
Femur osteotomy II	74° C	2
Femur drilling II	106° C / 122° C	1 (femur) / 4 (sawblade)
Tibia Osteotomy II	30° C	2
Cementation	26-28°C / 127° C	1,2,4 (bone interface) / 3 (surface of reference ball)

Table 4 Excerpt of Temperature Values recorded during Implantation Procedure

6.1.2 Heating related to imaging

During the performed clinical imaging sequences no isolated heating of any of the overserved measurement points was recorded. The temperature fluctuated less than 1°C during the testing period of around two hours for each of the two tumor endoprostheses. This fluctuation was similar for both, the cemented and the uncemented MUTARS tumor endoprosthesis.
However, over the whole test span of more than 4 hours, the temperature in the examination room increased by around 1,5°C, a value negligible for the quality of the measurements themselves, but this shift in ambient temperature was identifiable in the data and resulted in bias as the second endoprosthesis tested (MUTARS cemented) was recorded with higher overall temperatures than the first one.

6.2 Phantom Testing

6.2.1 Radiofrequency induced heating

Data obtained during the tests for radiofrequency induced heating showed slight differences between sensors 1-3. No isolated increase in temperature for any of the given temperature probes was recorded.
The overall difference in temperature before and after the 15-minute-worst-case scenario across all prostheses was under 0.5°C. A slight fluctuation of temperature across all temperature probes (including the reference probe) during the experiment was recorded.
This statement was true for all the tumor endoprostheses.

With the mean value of the three temperature probes 1-3 compared against the reference temperature probe, no increase in overall temperature across the tumor endoprostheses were observed. An additional reference run was also performed where only the supporting structure without a tumor endoprosthesis and with similarly placed temperature probes underwent the same 15-minute sequence with 2W/kg of SAR procedure.

The results from the 15-minute “worst-case-scenario” are displayed below using descriptive statistics as well as using a graphical depiction of the temperature probes 1-3 and the

reference probe. All temperatures are given in degree Celsius. The graphs show rounded values (rounded to the first decimal) and one data point every 30 seconds for better visual depiction. Descriptive statistics were performed for 180 values without rounding for each of the tested tumor endoprostheses and sensors.

6.2.1.1 GMRS

The GMRS tumor endoprosthesis showed very slight fluctuations in temperature, with the highest recorded ΔT at the distal femoral stem of 0,34°C.

	Minimum Temperature	Maximum Temperature	Median Temperature	Standard Deviation	ΔT
Temp 1	22,54	22,88	22,7127	,06283	0,34
Temp 2	23,00	23,29	23,1471	,05919	0,29
Temp 3	23,10	23,36	23,2333	,05311	0,26
Reference	22,59	22,89	22,7364	,05332	0,30

Table 5 Descriptive Statistics of GMRS Tumor Endoprosthesis Temperature Values

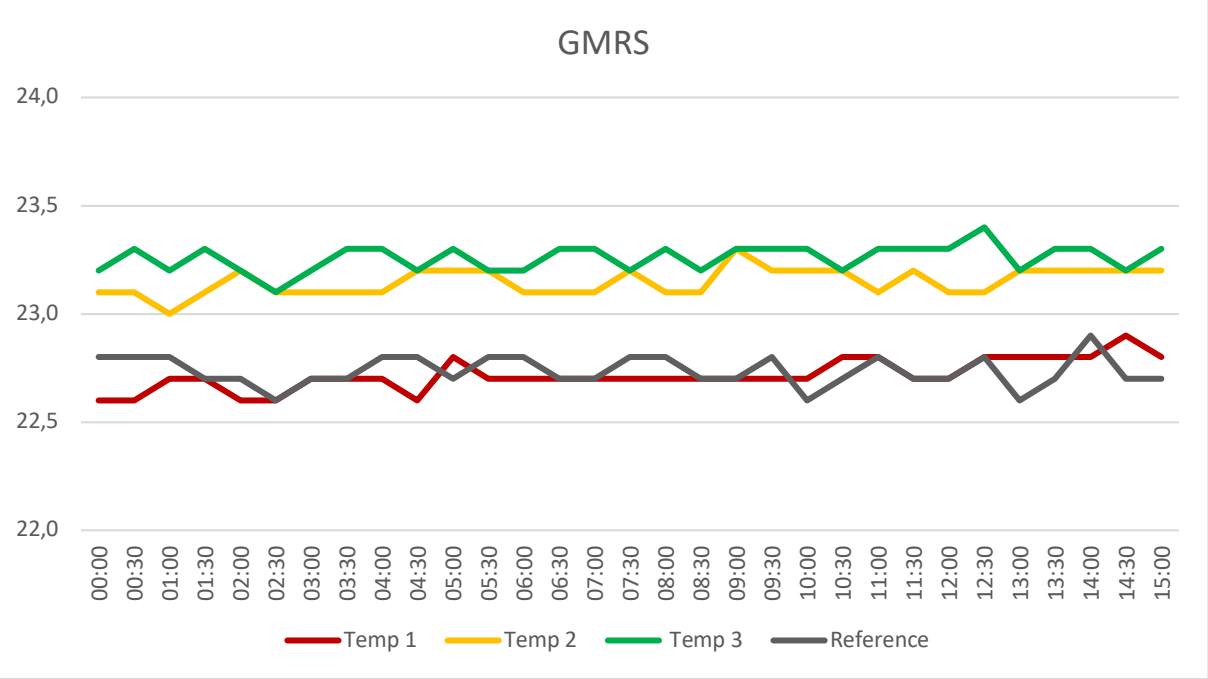

Fig. 9 GMRS Values Organized

6.2.1.2 LPS

LPS showed slightly greater variation in temperature than GMRS, with a maximum ΔT at the articulating joint of 0,48°C over the course of 15 minutes.

	Minimum Temperature	Maximum Temperature	Median Temperature	Standard Deviation	ΔT
Temp 1	23,01	23,36	23,1842	,07376	0,35
Temp 2	22,54	22,92	22,7517	,07084	0,48
Temp 3	23,34	23,75	23,5250	,08928	0,41
Reference	22,90	23,18	23,0716	,05759	0,28

Table 6 Descriptive Statistics of LPS Tumor Endoprosthesis Temperature Values

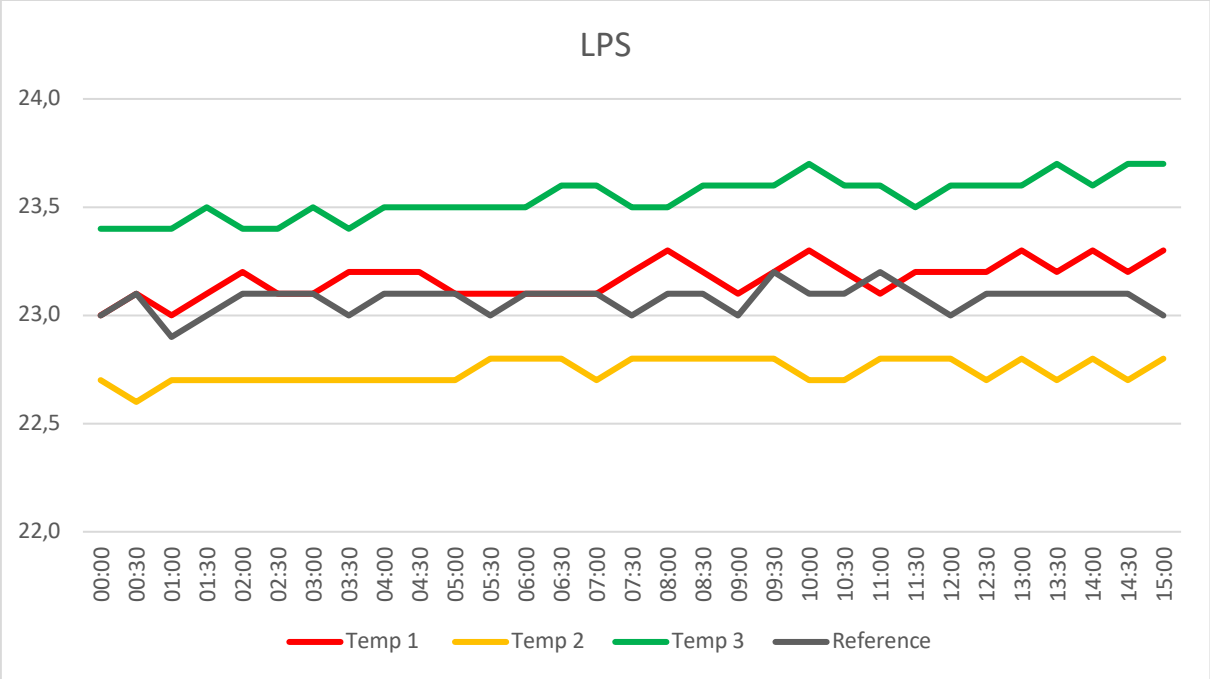

Fig. 10 LPS Values Organized

6.2.1.3 MUTARS

The MUTARS tumor endoprosthesis showed the largest differences in temperature in the proximal tibial stem like the MUTARS uncemented variety with a ΔT of 0,44°C.

	Minimum Temperature	Maximum Temperature	Median Temperature	Standard Deviation	ΔT
Temp 1	23,19	23,54	23,3718	,07198	0,35
Temp 2	22,77	23,14	22,9585	,06718	0,37
Temp 3	23,22	23,66	23,4751	,08408	0,44
Reference	22,92	23,18	23,0334	,04566	0,26

Table 7 Descriptive Statistics of MUTARS cemented Tumor Endoprosthesis Temperature Values

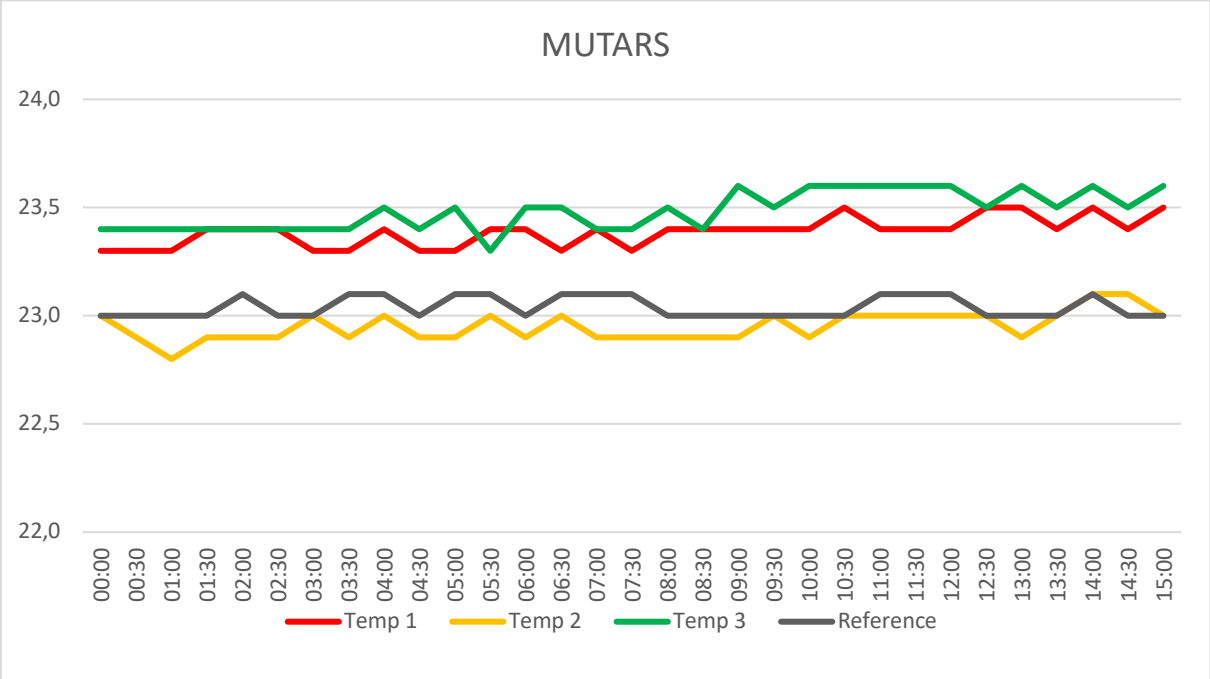

Fig. 11 MUTARS Values Organized

6.2.1.4 Reference Run

The reference run without an added tumor endoprosthesis but rather only the testing setup configured with the sensors recording the temperature in a comparable area resulted in a maximum ΔT of 0,48°C at temperature probe 2 which would have recorded the articulating joint in the other setups.

	Minimum Temperature	Maximum Temperature	Median Temperature	Standard Deviation	ΔT
Temp 1	22,60	22,86	22,7388	,04988	0,26
Temp 2	23,23	23,71	23,5467	,06988	0,48
Temp 3	22,99	23,31	23,1275	,05158	0,32
Reference	22,43	22,77	22,6366	,05377	0,34

Table 8 Descriptive Statistics of Reference Run without Tumor Endoprosthesis Temperature Values

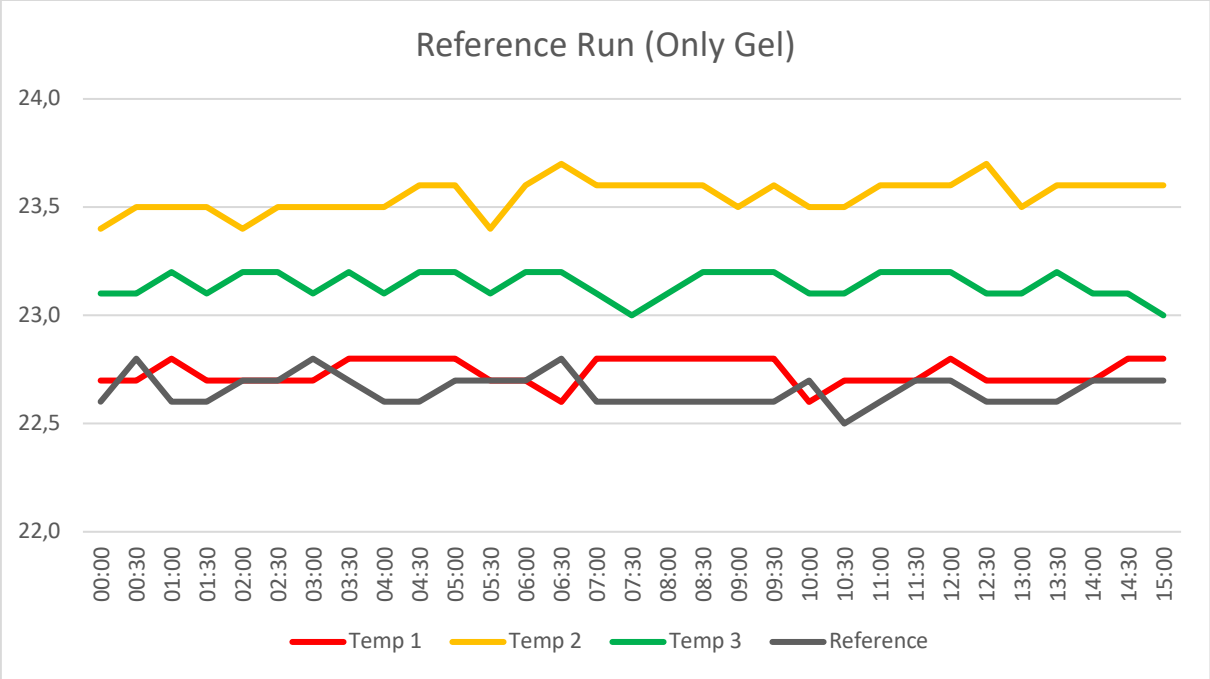

Fig. 12 Reference Run Values Organized

6.2.1.5 Mean of Temperature Sensors 1-3 vs. Reference

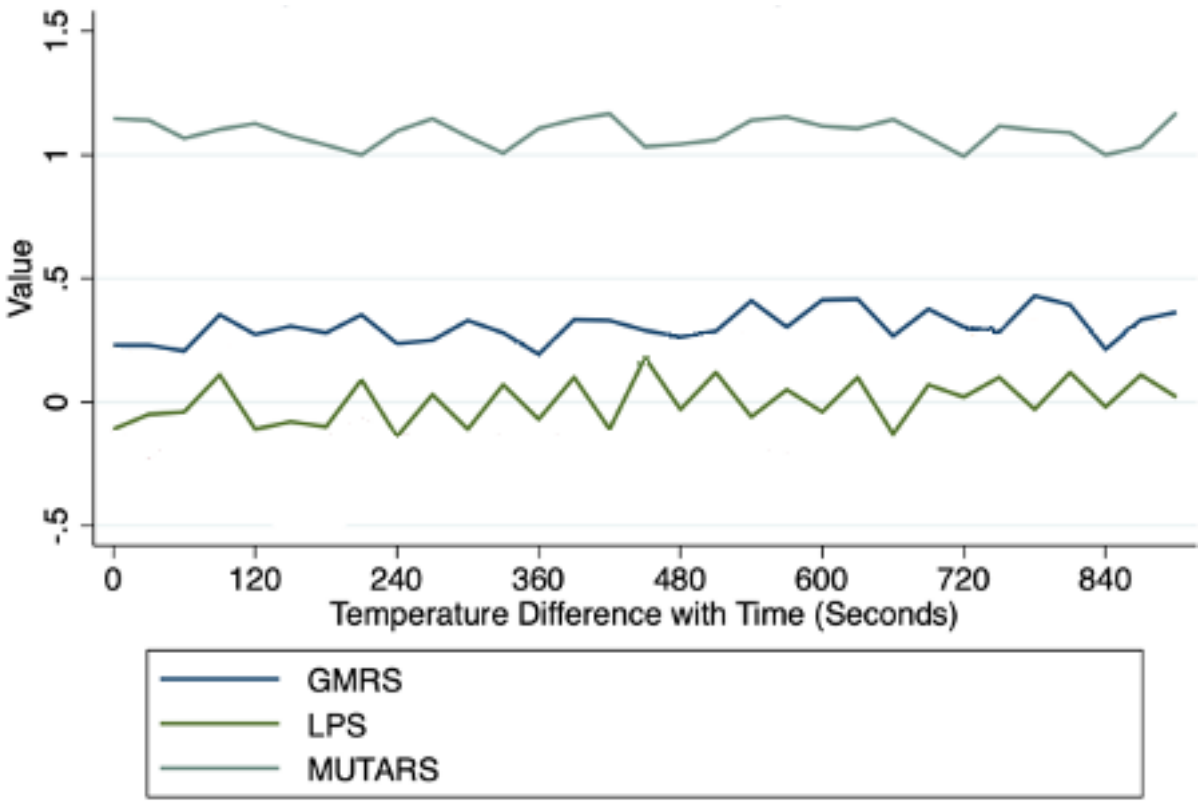

Fig. 13 Mean of Temp 1-3 of Test Runs vs. Reference

6.2.2 Displacement Force

The resulting angle of displacement resulting from the static B_0 field at the entrance of the bore proved to be between 4-5° angle of deflection for all the tested tumor endoprostheses. This displacement angle is consistent with other publications, where orthopedic devices made from titanium alloys showed overall similar displacement angles.[39]

The calculated forces resulting from the static magnetic field are presented in the following table:

Implant	Weight (g)	Deflection angle (°)	Displacement force (N)
MUTARS	1256	4	0,86
GMRS	1315	5	1,13
LPS	1392	4	0,96

Table 9 Displacement Force

The greatest displacement force was calculated to be 1,13N or 113g of force for the Stryker tumor endoprosthesis. The lowest calculated displacement force was observed with 0,72N or 72g of force for the MUTARS tumor endoprosthesis.

The induced torque we observed during our tests would be equivalent to a 2 (slow and moderate alignment) on a numerical scale of 1-4 as is used in other publications[39], however we did not measure the resulting magnetically induced torque using any of the possible methods stated in the ASTM guidelines, as the torque we observed did not have a significant effect on the tumor endoprostheses.

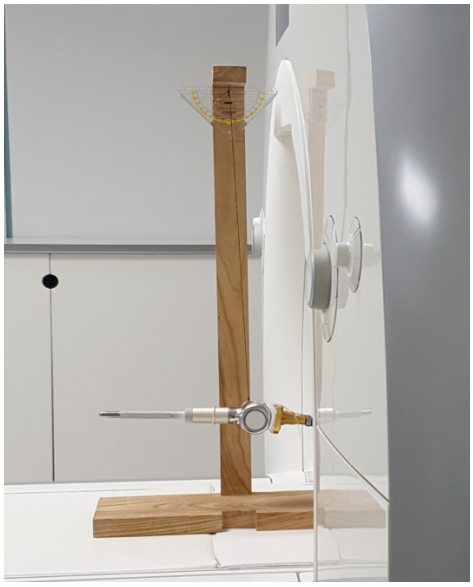

Fig. 14 Tumor Endoprosthesis (MUTARS) with displacement angle of 4°. Slow and moderate alignment with the magnetic field lines observed

6.2.3 Quality of images produced

The focus of this thesis was to evaluate the amount if interface between tumor endoprostheses and magnetic resonance fields regarding patient's safety during standard clinical imaging procedures. Therefore, a further analyzation of the quality of images produced was outside the scope of this thesis.

However, the images resulting from standard protocols as well as "metal artifact suppression" sequences, which are usually performed to increase the diagnostic value of MR images, showed considerable artifacts. The extent to which the tumor endoprostheses caused susceptibility artifacts did not differ drastically for the different endoprostheses.

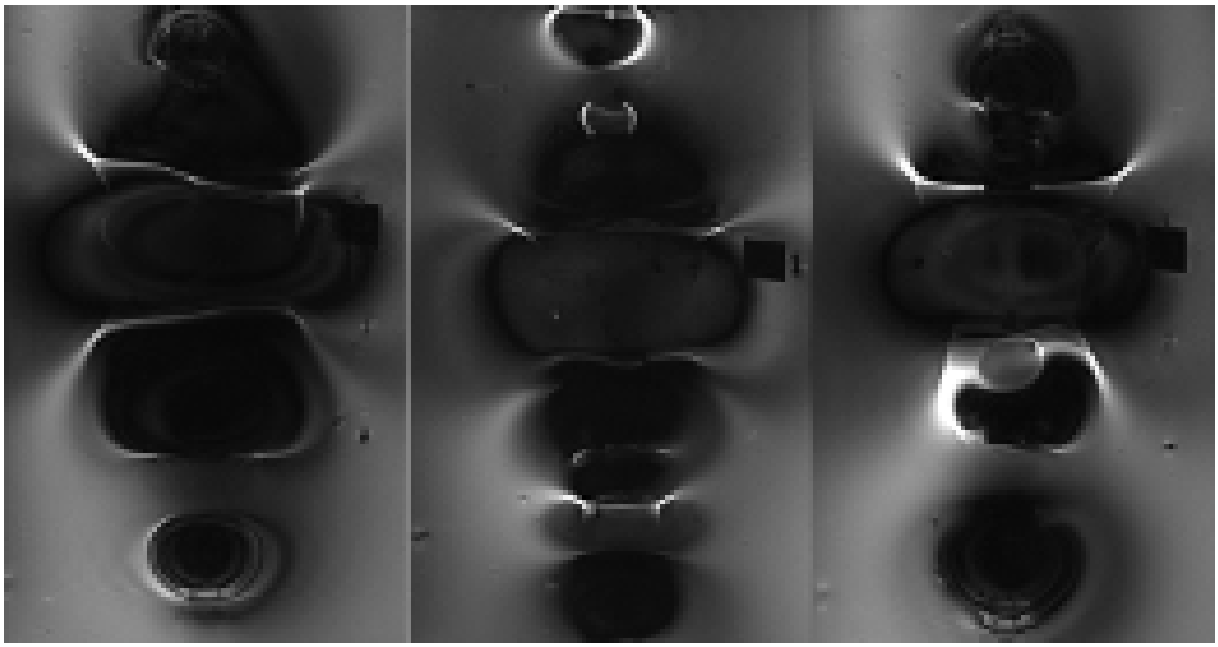

Fig. 15 Susceptibility Artifacts (T1 TSE) Left to Right: LPS, MUTARS, GMRS

7 Discussion

This study showed that several of the surgical techniques used to perform limb salvage surgery and the implantation of tumor endoprostheses causes a major increase in temperature at and around the implantation site. This change in temperature could potentially pose a risk to the bone due to thermal bone necrosis which could in turn affect the hold of the implant and could contribute to aseptic loosenging. This is of great concern, as the structural integrity of the bony supports is necessary to provide sufficient hold for the tumor endoprostheses.
This is consistent with several other publications, which also showed that the use of power tools and especially drills must be done thoughtfully as to not reach critical temperatures.
To overcome this threat to the bone and subsequent risk of aseptic loosening of the endoprosthesis, frequent cooling as well as lower feeding speeds of the tool as well as lower revolutions per minute (short RPM) could be utilized.[40]
All these measures would result in a generally lower increase in temperature.
This part of the study had a limitation: we performed our tests with cadavers which have a considerably lower ambient temperature of around 21° C, with the overall increase in temperature being more important than the ultimately reached temperature.
The heating effects observed during this cadaver study could therefore be even greater in-vivo.

Certainly, additional factors need to be considered, as cadavers have no active blood flow, which could provide a cooling effect at the affected area. However, we did not put an emphasis on the evaluation of the risks during the implantation procedure and possible threat prevention. A thoughtful approach to the use of power tools is advisable in any case.

Measurements of the heating of bone cement during hardening displayed large increases in temperature in the reference ball with minimal changes in temperature at the implantation site. This is most likely due to the relatively thin layer of bone cement surrounding the implanted stem when compared to the reference ball.

The bone cements in clinical use are mostly PMMA (polymethylmethacrylate) and harden via polymerization in an exothermic reaction which is known to increase the temperature of surrounding tissue.[41] The increase in temperature seems to be related to the thickness of reacting material as well as its shape. While the material around the stem is thin and flat, the overall surface area in relation to the amount of reactive material is large, apparently providing sufficient cooling area to negate the potential risk of dangerously increased temperature over the critical temperature for thermal bone necrosis. The reference ball on the other hand did heat up considerably, which can be attributed to the increased thickness as well as the shape of the ball, as a round spherical body has the least amount of surface for any given volume.

With the cement thicknesses in clinical being around 1.0-1.5mm[42], the hardening process would not result in a dangerous increase in temperature in the surrounding bone tissue in our tests.

In our study we observed the change in temperature in a cadaver, which has no active blood flow. In theory, the prevalence of active cooling measures like blood flow could keep temperatures even lower due to the higher heat capacity of water compared to air.

The recorded in-situ temperatures during our experiment would most likely not be a threat to the bone integrity.

Nevertheless, a precise analyzation of the effects of bone cement hardening and potential risks to bone tissue was not the main objective of this thesis, as this topic has been subject to numerous publications, in-vitro and in-vivo testing as well as subject of different computer generated models.[43–45]

The clinical imaging protocols performed of the cadaver legs with the implanted tumor endoprostheses did not show an isolated increase in temperature at any of the observed test

locations. This statement is true for both, the cemented as well as the uncemented MUTARS tumor endoprosthesis. The addition of a knee coil over the implant did not alter the results. Although an overall increase in temperature around the endoprostheses during the test procedure was observed, this can be attributed to the overall increase in ambient temperature in the examination room over the time span of eight hours.
The temperature within the examination room was well within specification of the ASTM protocols, which specify a room temperature stability of a change of less than 1° C within one hour.

The cadaver experiments had some limitations. We only performed the implantation procedure with MUTARS tumor endoprostheses and the appropriate instrumentation. Additionally, only one configuration of stem length (distal femur as well as proximal tibia) and only one length for the extension pieces for cemented and uncemented endoprostheses was tested. Therefore, not every possible length configuration was adequately represented in our study.

During the cadaver imaging procedures, no reference probe was used, as all four available fluoroptic temperature probes were recording the temperature at the interfaces and the tumor endoprostheses specifically. Regardless, this experiment showed no clinically relevant increase in temperature in and around the tumor endoprostheses.
Therefore, it can be assumed that standard clinical imaging of the implantation site as well as standard clinical imaging of any other body regions of patients who have undergone implantation of a MUTARS tumor endoprosthesis does not pose a risk to the patients due to excessive heating effects attributed to radiofrequency induced heating.

The tests for radiofrequency induced heating using a standardized phantom and a testing protocol did not show an isolated increase in temperatures at any of the given testing locations.
In addition to the “15-minute-worst-case-scenario“ sequences, we also performed standard clinical protocols for hip and knee imaging using different TSE, TIRM and VIBE-DIXON sequences.
None of our tests showed any fluctuation of temperature for the testing period of more than 0,5° C. This change in temperature is very comparable to the normal daily change in body

temperature in healthy adults and is not expected to cause any detrimental effects for the patient.[46]

As with the cadaver study, no active cooling through blood flow or a circulation pump was in place. The role and extent to which this cooling effect would affect the resulting temperature around the metal was not part of this thesis, however it can be expected that the resulting fluctuation in temperature would be even lower as any energy deposition in the tissue and the prostheses would immediately be transported away from the imaging site.

The maximum ΔT recorded with a tumor endoprosthesis was 0,48°C for temperature probe 2 for the LPS. A comparable ΔT was recorded during the reference run without a tumor endoprosthesis in place. This change in temperature can therefore not easily be attributed to heating effects of the tumor endoprosthesis but rather to variations in the sensors over the test span.
Supporting this theory is that radiofrequency induced heating effects would most likely occur at the ends of the stems as mentioned in the introduction and not at the articulating joints. Even if this ΔT was the result of radiofrequency induced heat deposition, it would be a subordinate safety concern for the patient.

With the mean value of temperature probes 1-3 compared to the reference probe, the associated graphs would show a rise along the y-axis if any of the temperature probes 1-3 did portray an increase in temperature during the test.

Multiple limitations of our experiment must be considered:

Firstly, only modular tumor endoprostheses systems from three different manufacturers were used. There are many more systems available worldwide, with different manufacturers potentially using different alloy compositions, which could potentially result in an overall different outcome.

Secondly, we only performed one test cycle per tumor endoprosthesis as well as only one length configuration.

Results could be different for different length configurations, as resonance effects with the radiofrequency field depend on the length of the metal in relation to the excitation frequency of the MRI apparatus in use. The absence of any clinically relevant heating effects however would lead us to believe that more test repetitions as well as more length configurations wouldn´t have changed the outcome considerably.

Thirdly, ultrasonic gel was used as filling for the phantom instead of the saline gelatin formulated in the ASTM protocols for better shelf live. As the conductive properties of the ultrasonic gel are relatively close bodily tissue and the recorded change in temperature is low, we would not expect a drastic change in outcome with another formula of gelatin.

The experiment evaluating the amount of magnetic displacement force revealed that the displacement force exerted by the static B_0 field is around or lower than 1/10 of the weight of the tumor endoprostheses, with a maximum calculated displacement force of around 113g with a tumor endoprosthesis weight of 1315g.
Thus, the displacement forces occurring during magnetic resonance imaging can be considered negligible according to the ASTM protocol.[47] This is due to the fact the earths gravitational field exerts a constant force onto the tumor endoprosthesis resulting in its measured mass.
Therefore, only displacement forces of more than the weight of the endoprostheses pose a relevant additional risk during magnetic resonance imaging. Forces that would need additional evaluation would result in angles of displacement of more than 45° in this test, a multiple of the displacement angles that were observed, with the greatest angle of displacement being 5°.

The calculated angles of displacement are comparable with other publications, where titanium implants showed displacement angles of 0°-7°[39,48], depending on the strength of the MRI apparatus (1.5 T vs. 3 T). The reported angles of deflection for cobalt-chromium steel implants on the other hand vary considerably from 1° to 45°.[39]

This could be a source of concern, as the articulating joints of the tested tumor endoprosthesis systems are made from chromium molybdenum steel alloys.

However, as the tested tumor endoprostheses would in most cases be configured in the tested configuration with proximal and distal titanium stems instead of a singular chromium molybdenum steel module, we would expect our test results to be more representative to the in vivo effect on the implanted device during magnetic resonance imaging in a standard clinical setup.
In addition, the magnetic properties of a body made out of different materials with different magnetic properties should be described as a vector resulting from the main magnetic momentum of the body, not of individual parts of this body.[14]

Although we did not quantify the amount of torque exerted by the magnetic resonance fields, we did observe moderate and slow alignment with the magnetic field lines of the B_0 field.
On a numerical scale from 1-4 which has been utilized by other authors[39], this would be considered a 2 comparable to other sources which have evaluated the induced torque of titanium alloy orthopedic implants.[39]
As mentioned in the introduction however, the extent to which metallic devices exert force on the surrounding tissue largely depends on the length, with it counterintuitively being lower with longer devices.[10]
Therefore, the induced torque can be considered negligible and not a safety hazard during standard clinical magnetic resonance imaging.

For this experiment some of the same limitations must be considered as for radiofrequency induced heating.
We did only evaluate the amount of displacement force for one configuration per manufacturer.
Furthermore, we oriented the tumor endoprostheses horizontally, as we assumed this would result in more realistic and clinically relevant results.

In addition, the resulting angle of deflection was read of by different individuals from a protractor. Therefore, the possibility for slight variation of the read angle from the actual angle cannot be dismissed, but as the mean angle of three different observations was used for calculation, we would not expect this to meaningfully affect the results.

Additionally, the allowed margin for error is considerable, with at least 45° angle of displacement being necessary to be of relevant concern.

The main reason for our study was to evaluate if magnetic resonance imaging poses a threat to the patient's wellbeing or the hold of the endoprosthesis.
Therefore, we did not further evaluate if the images obtained via such imaging procedures are of any diagnostic worth.
It must be noted however that the images being produced during standard clinical imaging protocols as well as the metal artifacts suppression protocols are relatively poor in quality, as there are many alterations around the tumor endoprostheses in the images due to susceptibility artifacts.
Thus, the potential diagnostic value of magnetic resonance imaging directly at or close to the implantation site must be evaluated closely. For reference see Fig. 17, black aspects in the pictures are voxels which couldn't be used for rendering of a 2D image. Adjacent structures similarly can be "blacked" out in-vivo imaging.

7.1 Conclusion

In summary, our results suggest that the tested tumor endoprostheses are safe for the magnetic resonance imaging environment. Patients who have undergone implantation of these devices can therefore be admitted to such imaging procedures without excessive risks due to interactions of the implanted tumor endoprosthesis with the magnetic resonance fields.

As the images resulting from imaging of the directly affected implantation sites are subject to reduced image quality due to artifacts around the prostheses, the benefit of these procedures must be evaluated closely as local recurrences might not be detectable using this imaging technique. We would expect that magnetic resonance imaging procedures at any anatomical site can be performed safely.

8 Bibliography

1. Strauss, S. J. *et al.* Bone sarcomas: ESMO–EURACAN–GENTURIS–ERN PaedCan Clinical Practice Guideline for diagnosis, treatment and follow-up. *Ann. Oncol.* **32**, 1520–1536 (2021).
2. Fornetti, J., Welm, A. L. & Stewart, S. A. Understanding the Bone in Cancer Metastasis. *J. Bone Miner. Res.* **33**, 2099–2113 (2018).
3. Tavare, A. N. *et al.* Postoperative Imaging of Sarcomas. *Am. J. Roentgenol.* **211**, 506–518 (2018).
4. Takeuchi, A., Lewis, V. O., Satcher, R. L., Moon, B. S. & Lin, P. P. What Are the Factors That Affect Survival and Relapse After Local Recurrence of Osteosarcoma? *Clin. Orthop.* **472**, 3188–3195 (2014).
5. Xu, M., Wang, Z., Yu, X., Lin, J. & Hu, Y. Guideline for Limb-Salvage Treatment of Osteosarcoma. *Orthop. Surg.* **12**, 1021–1029 (2020).
6. Zou, C. *et al.* Long-term outcomes of limb salvage treatment with custom-made extendible endoprosthesis for bone sarcoma around the knee in children. *J. Orthop. Surg.* **15**, 14 (2020).
7. Khan, I., Gerrand, C. & Saifuddin, A. Imaging following surgery for primary appendicular bone tumours. *Skeletal Radiol.* **50**, 1527–1555 (2021).
8. Winn, N. & Lalam, R. Imaging of the Knee and Surrounding Structures Following Tumor Surgery. *Semin. Musculoskelet. Radiol.* **22**, 481–505 (2018).
9. Schick, F. Grundlagen der Magnetresonanztomographie. *Radiol.* **47**, S7–S26 (2007).
10. Panych, L. P. & Madore, B. The physics of MRI safety: Physics of MRI Safety. *J. Magn. Reson. Imaging* **47**, 28–43 (2018).
11. U.S. Department of Health and Human Services Food and Drug Administration Center for Devices and Radiological Health. Testing and Labeling Medical Devices for Safety in the Magnetic Resonance (MR) Environment. (2021).
12. Kraff, O. & Quick, H. H. Sicherheit von Implantaten im Hochfeld- und Ultrahochfeld-MRT. *Radiol.* **59**, 898–905 (2019).
13. Tsukimura, I. *et al.* Assessment of magnetic field interactions and radiofrequency-radiation-induced heating of metallic spinal implants in 7 T field: ULTRAHIGH-FIELD EFFECTS ON METALLIC IMPLANTS. *J. Orthop. Res.* **35**, 1831–1837 (2017).
14. Dössel, O. *Bildgebende Verfahren in der Medizin*. (Springer Berlin Heidelberg, 2016). doi:10.1007/978-3-642-54407-1.
15. Schick, F. MRT – Wechselwirkungen mit magnetisch aktivem und elektrisch leitfähigem Material. *Radiol.* **59**, 860–868 (2019).
16. Sammet, S. Magnetic resonance safety. *Abdom. Radiol.* **41**, 444–451 (2016).
17. Winter, L., Seifert, F., Zilberti, L., Murbach, M. & Ittermann, B. MRI-Related Heating of Implants and Devices: A Review. *J. Magn. Reson. Imaging* **53**, 1646–1665 (2021).
18. Kumar, R., Kumar, M., Malhotra, K. & Patel, S. Primary Osteosarcoma in the Elderly Revisited: Current Concepts in Diagnosis and Treatment. *Curr. Oncol. Rep.* **20**, 13 (2018).
19. Ritter, J. & Bielack, S. S. Osteosarcoma. *Ann. Oncol.* **21**, vii320–vii325 (2010).
20. Jackson, T. M., Bittman, M. & Granowetter, L. Pediatric Malignant Bone Tumors: A Review and Update on Current Challenges, and Emerging Drug Targets. *Curr. Probl. Pediatr. Adolesc. Health Care* **46**, 213–228 (2016).
21. Balamuth, N. J. & Womer, R. B. Ewing's sarcoma. *Lancet Oncol.* **11**, 184–192 (2010).

22. Grünewald, T. G. P. *et al.* Ewing sarcoma. *Nat. Rev. Dis. Primer* **4**, 5 (2018).
23. Messerschmitt, P. J., Garcia, R. M., Abdul-Karim, F. W., Greenfield, E. M. & Getty, P. J. Osteosarcoma: *J. Am. Acad. Orthop. Surg.* **17**, 515–527 (2009).
24. Whelan, J. S. *et al.* EURAMOS-1, an international randomised study for osteosarcoma: results from pre-randomisation treatment. *Ann. Oncol. Off. J. Eur. Soc. Med. Oncol.* **26**, 407–414 (2015).
25. Fritz, J. *et al.* Imaging of Limb Salvage Surgery. *Am. J. Roentgenol.* **198**, 647–660 (2012).
26. Morris, C. D., Wustrack, R. L. & Levin, A. S. Limb-Salvage Options in Growing Children with Malignant Bone Tumors of the Lower Extremity: A Critical Analysis Review. *JBJS Rev.* **5**, e7–e7 (2017).
27. Anagnostakos, K. & Kohn, D. Megaendoprothesen am Kniegelenk. *Orthop.* **39**, 949–959 (2010).
28. Niimi, R. *et al.* Prosthetic limb salvage surgery for bone and soft tissue tumors around the knee. *Oncol. Rep.* **28**, 1984–1990 (2012).
29. Schwartz, A. J., Kabo, M. J., Eilber, F. C., Eilber, F. R. & Eckardt, J. J. Cemented Distal Femoral Endoprostheses for Musculoskeletal Tumor: Improved Survival of Modular versus Custom Implants. *Clin. Orthop.* **468**, 2198–2210 (2010).
30. Henderson, E. R. *et al.* Failure Mode Classification for Tumor Endoprostheses: Retrospective Review of Five Institutions and a Literature Review. *J. Bone Jt. Surg.* **93**, 418–429 (2011).
31. Kaste, S. C., Neel, M. N., Rao, B. N., Thompson, V. F. & Pratt, C. B. Complications of limb-sparing procedures using endoprosthetic replacements about the knee for pediatric skeletal sarcomas. *Pediatr. Radiol.* **31**, 62–71 (2001).
32. Houdek, M. T. *et al.* Long term outcomes of cemented endoprosthetic reconstruction for periarticular tumors of the distal femur. *The Knee* **23**, 167–172 (2016).
33. Carr, A. J. *et al.* Knee replacement. *The Lancet* **379**, 1331–1340 (2012).
34. Pala, E. *et al.* Megaprosthesis of the knee in tumor and revision surgery. *Acta Bio-Medica Atenei Parm.* **88**, 129–138 (2017).
35. Grimer, R. J. *et al.* Very long-term outcomes after endoprosthetic replacement for malignant tumours of bone. *Bone Jt. J.* **98-B**, 857–864 (2016).
36. Kotz, R. Megaprothesen: KMFTR® bis GMRS®. *Orthop.* **39**, 922–930 (2010).
37. Bergovec, M. *et al.* Epidemiology of musculoskeletal tumors in a national referral orthopedic department. A study of 3482 cases. *Cancer Epidemiol.* **39**, 298–302 (2015).
38. ASTM International. Standard Test Method of Radiofrequency Induced Heating On or Near Passive Implants DUring Magnetic Resonance Imaging. (2011).
39. Mosher, Z. A., Sawyer, J. R. & Kelly, D. M. MRI Safety with Orthopedic Implants. *Orthop. Clin. North Am.* **49**, 455–463 (2018).
40. Mediouni, M. *et al.* Optimal parameters to avoid thermal necrosis during bone drilling: A finite element analysis: 3D DRILLING SIMULATION. *J. Orthop. Res.* **35**, 2386–2391 (2017).
41. Samad, H. A., Jaafar, M., Othman, R., Kawashita, M. & Razak, N. H. A. New bioactive glass-ceramic: Synthesis and application in PMMA bone cement composites. *Biomed. Mater. Eng.* **21**, 247–258 (2011).
42. Terrier, A., Büchler, P. & Farron, A. Bone–cement interface of the glenoid component: Stress analysis for varying cement thickness. *Clin. Biomech.* **20**, 710–717 (2005).
43. Stańczyk, M. & van Rietbergen, B. Thermal analysis of bone cement polymerisation at the cement–bone interface. *J. Biomech.* **37**, 1803–1810 (2004).
44. Boner, V., Kuhn, P., Mendel, T. & Gisep, A. Temperature evaluation during

PMMA screw augmentation in osteoporotic bone-An *in vitro* study about the risk of thermal necrosis in human femoral heads. *J. Biomed. Mater. Res. B Appl. Biomater.* **90B**, 842–848 (2009).
45. Li, C. *et al.* Finite Element Thermal Analysis of Bone Cement for Joint Replacements. *J. Biomech. Eng.* **125**, 315–322 (2003).
46. Brenner, B. *Physiologie*. (Georg Thieme Verlag, 2014).
47. ASTM International. Standard Test Method of Magnetically Induced Displacement Force on Medical Devices in the Magnetic Resonance Environment. (2015).
48. Zou, Y., Chu, B., Wang, C. & Hu, Z. Evaluation of MR issues for the latest standard brands of orthopedic metal implants: Plates and screws. *Eur. J. Radiol.* **84**, 450–457 (2015).